THE JOURNAL OF PHYSICAL CHEMISTRY LETTERS
A JOURNAL OF THE AMERICAN CHEMICAL SOCIETY

pubs.acs.org/JPCL Letter

# Elucidating Trivalent Ion Adsorption at Floating Carboxylic Acid Monolayers: Charge Reversal or Water Reorganization?

Srikanth Nayak, Raju R. Kumal, Seung Eun Lee, and Ahmet Uysal*

Cite This: J. Phys. Chem. Lett. 2023, 14, 3685−3690 Read Online

ACCESS | Metrics & More | Article Recommendations | Supporting Information

**ABSTRACT:** We study the adsorption of trivalent neodymium on floating arachidic acid films at the air−water interface by two complementary surface specific probes, sum frequency generation spectroscopy and X-ray fluorescence near total reflection. In the absence of background ions, neodymium ions compensate for the surface charge of the arachidic acid film at a bulk concentration of 50 $\mu$M without any charge reversal. Increasing the bulk concentration to 1 mM does not change the neodymium surface coverage but affects the interfacial water structure significantly. In the presence of a high concentration of NaCl, there is overcharging at 1 mM $Nd^{3+}$, i.e., 30% more $Nd^{3+}$ than needed to compensate for the surface charge. These results show that the total coverage of neodymium ions is not enough to describe the complete picture at the interface, and interfacial water and ion coverage needs to be considered together to understand more complex ion adsorption and transport processes.

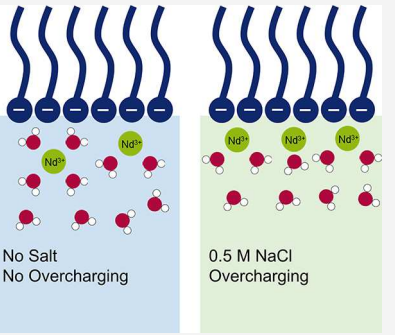




Ion adsorption and transport at charged interfaces are central to many important phenomena. Living cell membranes selectively transport ions.[1] Batteries transport ions through electrode surfaces.[2] The stability of colloids depends on the ions in the solution.[3] Chemical separations require selective ion adsorption and transfer.[4−13] A molecular scale understanding of ion−surface water interactions is crucial for addressing the key challenges in these fields.

In the classical picture of a charged interface, including Stern and diffuse layers of an electric double layer (EDL), the total charge of the counterions adsorbed at the interface cannot exceed the surface charge. However, in the past two decades, many experimental and theoretical studies have demonstrated that the charge of adsorbed ions can exceed the surface charge, leading to charge reversal or overcharging.[14−19] The origin of the overcharging can be chemical; i.e., specific interactions or chemical bonding between ions and the surface functional groups may lead to overcharging.[20] The overcharging may also originate from purely electrostatic interactions. Especially with multivalent ions, ion−ion correlations favor overcharging.[21,22] In highly concentrated solutions[23,24] or under an applied electric field,[25] overcharging may even happen with monovalent ions.

Floating surfactant layers at the air−aqueous interface (Langmuir monolayers) are useful model systems for studying ion adsorption and interfacial water at flat interfaces.[7−10,26−32] They provide a high charge density ($\leq$1 $e^-$/20 Å$^2$ or ∼0.8 C/m$^2$) for single-chain surfactants and are highly accessible to surface specific experimental probes. The most commonly used probes include sum frequency generation (SFG) spectroscopy, X-ray fluorescence near total reflection (XFNTR), and anomalous X-ray reflectivity (a-XR). XFNTR and a-XR provide a direct measure of the total number of interfacial ions exploiting the element specific X-ray absorption edge of the ions.[18,20] SFG spectroscopy provides an indirect measure of ion adsorption, through the changes happening to the interfacial water structure or the surface functional groups.[26,27,33]

Recently, Sthoer et al. reported an observation of overcharging of $Y^{3+}$ and $La^{3+}$ ions at arachidic acid (AA) monolayers with SFG spectroscopy.[27] The intensity of the -OH region signal (3200−3700 cm$^{-1}$) decreased as the bulk concentration increased from 100 nM to 10 $\mu$M, which is typical due to the decreasing surface charge and disturbed interfacial water organization. However, as the bulk concentration was increased further to 0.1 mM, the intensity of the SFG signal increased again. The increase in the intensity of the SFG signal has been interpreted as the overcharging of the interface by the adsorption of trivalent ions, causing a net electric field at the interface. Interestingly, in an earlier study with a very similar system, Wang et al. used XFNTR to show that $La^{3+}$ ions simply compensate for the surface charge by adsorbing at a 1:3 ratio.[20] This apparent contradiction can be due to an error in one (or both) of the measurements or a problem in the assumptions in the interpretation of data. As a third possibility, we hypothesize that our typical understanding

Received: January 25, 2023
Accepted: April 6, 2023
Published: April 10, 2023

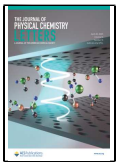





https://doi.org/10.1021/acs.jpclett.3c00225
J. Phys. Chem. Lett. 2023, 14, 3685−3690

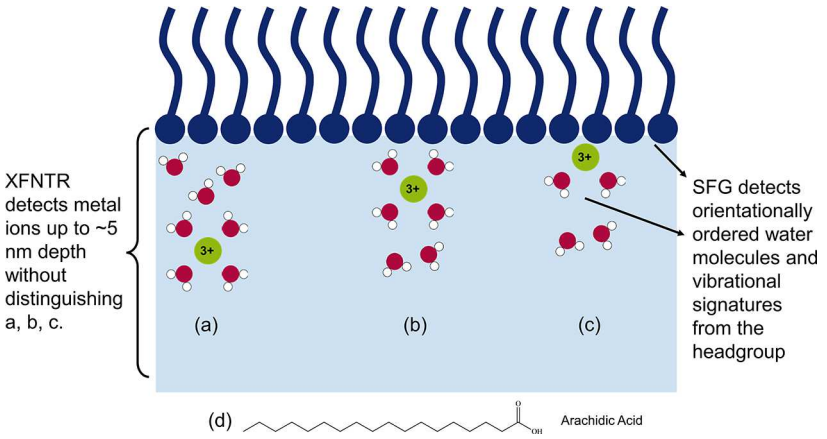


**Figure 1.** Schematic representation of possible adsorption of $Nd^{3+}$ ions at the interface. (a) $Nd^{3+}$ is multiple water layers from the interface. (b) $Nd^{3+}$ is in the Stern layer but fully hydrated. (c) $Nd^{3+}$ is partially dehydrated. XFNTR does not distinguish among cases a−c and provides the total number of ions within ~5 nm of the interface. SFG does not detect ions directly but detects their effects on interfacial water and surfactant headgroups. (d) Structure of arachidic acid.

of EDL is too simplistic and requires an improvement to explain both studies simultaneously. Also, the chemistry of the charged surface and the solution conditions, such as background salts, need to be considered carefully.

In this study, we utilize both SFG and XFNTR techniques to elucidate the adsorption of $Nd^{3+}$ at AA monolayers in detail and reconcile the apparent contradiction in the literature (Figure 1). By studying ion adsorption with and without background salts, we show that the -OH region SFG signal is not always an ideal probe for inferring ion adsorption, due to the ambiguity created by multiple effects, such as the hydration shell of the ions or interference effects.[30,34,35] On the contrary, XFNTR cannot provide some details of ion distribution, because it is sensitive to only the total number of ions in both Stern and diffuse layers and insensitive to the reorganization of ions between them.[28] Acknowledging the advantages and shortcomings of both methods allows the details of trivalent ion adsorption that cannot be determined by a single method to be elucidated.

Figure 2 shows the variation of the neodymium surface coverage at AA monolayers as a function of total Nd concentration ($[Nd]_t$) obtained by the corresponding XFNTR results (Figure S1). Nd coverage at the monolayer surface increases monotonically both with and without the background salt (NaCl). In the absence of NaCl, the surface coverage reaches saturation at a value of ~0.016 Nd/Å$^2$. This value agrees with the Nd coverage required for monolayer charge neutralization by $Nd^{3+}$ as there is 1 AA molecule per 20 Å$^2$. $Nd^{3+}$ is the predominant species in the bulk solution in the pH range of 5.5−6 used here. This value is also in agreement with the surface coverage obtained with $La^{3+}$ ions at 0.1 mM under a fully deprotonated AA monolayer.[20] We note that AA is reported to be mostly protonated on pure water with an apparent $pK_a$ of ~10.8,[30] but the apparent $pK_a$ of AA monolayers shifts to ~4 in the presence of lanthanides.[20]

In the presence of 0.5 M NaCl, when $[Nd]_t$ < 10 $\mu$M, the surface coverage of Nd species is decreased relative to the no-salt case, due to the competition between $Na^+$ and $Nd^{3+}$ (Figure 2). When $[Nd]_t$ = 0.1 mM, the surface coverage reaches ~0.016 Nd/Å$^2$. When $[Nd]_t$ = 1 mM in the solution, the surface coverage of Nd is ~0.022 Nd/Å$^2$, significantly higher than that expected for charge neutrality of AA headgroups by trivalent ions. Evidently, 0.5 M background

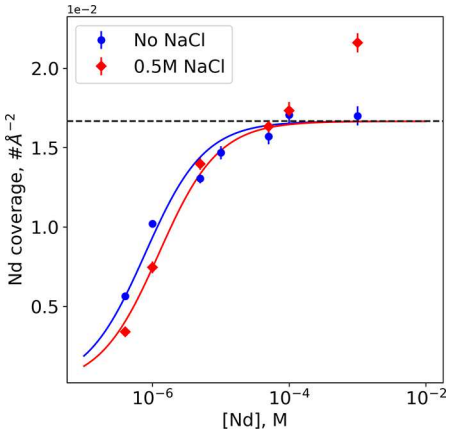


**Figure 2.** Variation of the number of Nd atoms per square angstrom of surface area with increasing $[NdCl_3]_t$ under an AA monolayer at $\pi$ = 10 mN/m, without any background salt (blue circles) and with 0.5 M NaCl (red diamonds). The solid lines are fits obtained with the Langmuir adsorption isotherm model. For complete coverage with charge balance of the surface with trivalent Nd species (1:3 Nd:AA), the surface density of Nd is 0.0166 Å$^{-2}$ (dashed line).

salt enhances the "salting out" of $Nd^{3+}$ ions, enabling overcharging that is not possible in the absence of background salt. This is especially important for chemical separation of rare earths, where highly concentrated solutions are typical under process conditions.[24] There is an interplay of interfacial hydration and adsorption of ions to the monolayers, which can be expected to play a major role especially in the case of strongly hydrated trivalent cations.[22,36] We next focus on SFG results under the same conditions.

Variation of the SFG spectra in the OH stretching region with increasing $[Nd]_t$ in water is shown in Figure 3a. The two bands roughly centered at wavenumbers of 3250 and 3550 cm$^{-1}$ are attributed to the relatively more strongly and weakly hydrogen-bonded water molecules, respectively.[33] At a relatively low $[Nd]_t$ of 400 nM, the OH region is significantly affected with a near uniform drop in the bimodal intensities. From the XFNTR results (Figure 2), this corresponds to ~$^1/_3$ coverage of $Nd^{3+}$ species. As the $Nd^{3+}$ coverage increases to that required for full charge compensation, when $[Nd]_t$ ~ 10 $\mu$M, the OH region is nearly flat with a total loss of the typical


https://doi.org/10.1021/acs.jpclett.3c00225
J. Phys. Chem. Lett. 2023, 14, 3685−3690

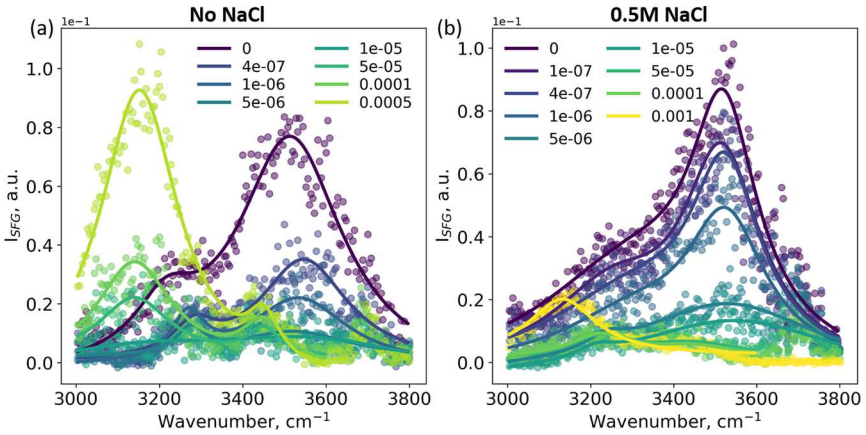


**Figure 3.** Variation of the SFG spectra corresponding to the OH stretching vibrations with increasing $[Nd]_t$ (a) without a NaCl background and (b) with a 0.5 M NaCl background. Solid lines through the scattered data are fits obtained by combination of two Lorentzian peaks. Legend entries refer to the $[Nd]_t$ in the system. All of the spectra were recorded under SSP polarization combination.

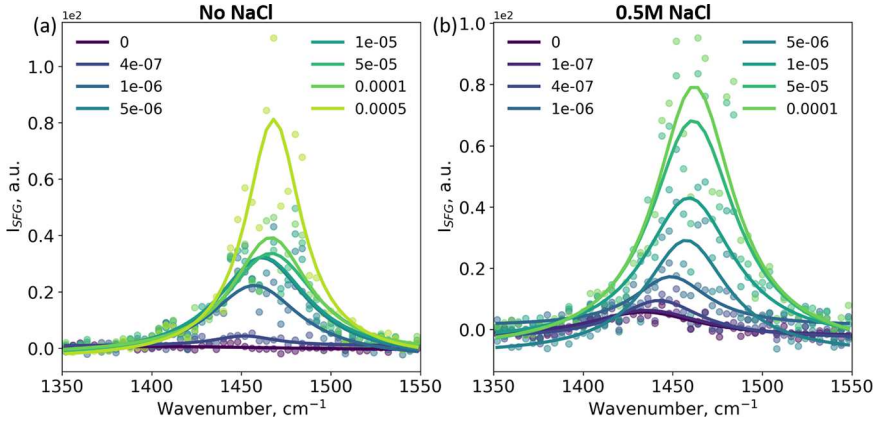


**Figure 4.** Variation of the SFG spectra corresponding to the $COO^-$ stretching vibrations with increasing $[Nd]_t$ (a) without a NaCl background and (b) with a 0.5 M NaCl background. Solid lines through the scattered data are fits obtained by Lorentzian peaks. Legend entries refer to the $[Nd]_t$ in the system. All of the spectra were recorded under SSP polarization combination.

bimodal feature of interfacial water. Interestingly, although the surface coverage of Nd species does not change with a further increase in $[Nd]_t$, the corresponding SFG shows a continual change in the OH region. At and above ~50 $\mu$M $[Nd]_t$, there is a prominent peak at ~3150 cm$^{-1}$ that is strengthened with increasing $[Nd]_t$. Simultaneous with the appearance of this 3150 cm$^{-1}$ peak is the appearance of two weaker peaks at ~3450 and 3700 cm$^{-1}$ (not modeled in the fits). Sthoer et al. have interpreted the appearance of these peaks as indications of "overcharging".[27] Our XFNTR results clearly negate this interpretation. We do not see any correlation between the overcharging and the appearance of these peaks as they are observed even without overcharging (Figure 3). In addition, the red-shift of the peaks with respect to the water/AA spectrum and the changes in the overall shape of the spectra (higher 3150 cm$^{-1}$ peak relative to the 3450 cm$^{-1}$ peak, as opposed to the higher 3550 cm$^{-1}$ peak relative to the 3250 cm$^{-1}$ peak in the water/AA spectrum) reflect complex changes in the interfacial hydration in the presence of Nd species, rather than reorientation of water molecules due to the reversal of the surface charge.

In the presence of 0.5 M NaCl, the OH region is affected differently by the adsorption of $Nd^{3+}$ to the monolayer (Figure 3b). Without $Nd^{3+}$ in the solution, the OH region looks qualitatively similar, although the peak intensities are different, to the corresponding spectra in the water/AA system (violet trace in Figure 3a), as has been previously reported.[37] Studies with varying NaCl concentrations under AA monolayers have posited that the weak signal in the water/AA system, which is comparable to a very high ionic strength system, is due to the destructive interference of the SFG signal coming from the sample depth.[30,34] The persistence of the OH signal at very high NaCl concentrations has been attributed to the finite size of the counterion ($Na^+$), which limits the charge screening when the debye length is low.[37]

With the addition of $NdCl_3$ to the subphase, the intensities of bands at 3250 and 3550 cm$^{-1}$ decrease gradually in contrast to the immediate decrease in the absence of the background salt (Figure 3b). When $[Nd]_t$ = 1 mM, a peak appears at ~3150 cm$^{-1}$, similar to the no-salt condition but with a relatively lower intensity. We note that at this highest concentration of $Nd^{3+}$ with a 0.5 M NaCl background, the $Nd^{3+}$ ions indeed overcharge the interface (Figure 2). Therefore, the 3150 cm$^{-1}$ peak appears regardless of the overcharging and is actually weaker when overcharging happens. This shows that the resurgence of the OH stretching mode signal is not a good indicator of the Nd concentration at the surface. The OH region is significantly affected by solvent reorganization, in addition to ion adsorption, which prohibits


https://doi.org/10.1021/acs.jpclett.3c00225
J. Phys. Chem. Lett. 2023, 14, 3685−3690

us from drawing direct conclusions about the interfacial composition in terms of metal coverage.[38]

In addition to -OH vibrations of water, the symmetric stretching mode of the $COO^-$ group has been used to evaluate the ion−monolayer interactions with fatty acid monolayers.[26,27,30,37] Figure 4 shows the SFG spectra corresponding to this peak with and without the salt background. There is an increase in peak strength and a shift in peak position with increasing $[Nd]_t$ both with and without a salt background, though concentration-dependent trends are different. The spectral shape seems to match better with the results of Sthoer et al.[27] than with those of Sung et al.,[26] who report a bimodal peak shape that they attribute to a mix of bare $COO^-$ and the lanthanide−$COO^-$ complex. Sthoer et al. have studied the carboxylate stretching region thoroughly, modeling this region as a sum of three differing modes of carboxylate−lanthanide interactions.[27] Due to the low signal-to-noise ratio in our spectra, we have used a single peak to fit the data. This region is also affected by the CH and OH bending modes, further complicating quantitative analysis.[30] The peak amplitudes from the single Lorentzian fits are shown in Figure 5. In the absence

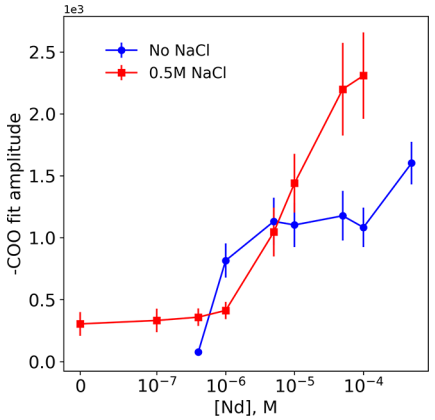


**Figure 5.** Variation of the fit amplitude in the -COO stretch region with increasing $[Nd]_t$ without a NaCl background (blue circles) and with a 0.5 M NaCl background (red squares). The connecting lines through the scattered data points are guides for presentation.

of the background salt, the peak amplitude is saturated around 1 $\mu$M but increases again at the highest concentration. In the presence of the background salt, the intensity of the signal increases continuously but with two different slopes, where the change in slope happens around 1 $\mu$M. In light of the XFNTR results, these changes in the $COO^-$ peak amplitudes indicate that the peak is affected by the deprotonation and reorientation of the $COO^-$ group.

When considered altogether, our results provide a detailed picture of $Nd^{3+}$ adsorption at AA monolayers. It is clear that electrostatic attraction can bring $Nd^{3+}$ ions to the interface even at very low bulk concentrations. However, the strongly hydrated $Nd^{3+}$ does not interact with the AA headgroup directly because it cannot shed the hydration shell. This leads to an adsorption that can be described as Figure 1a or 1b. The partial dehydration of $Nd^{3+}$ happens differently in the absence and presence of the NaCl background. We observe that the concentration-dependent trends in -OH and -COO SFG signals are more monotonic in the presence of NaCl (Figures 3b and 4b). In contrast, without any background salt, both signals show a large jump at very low concentrations and then remain relatively constant over a 100-fold change in the bulk $Nd^{3+}$ concentration (Figures 3a and 4a). However, the XFNTR trends that provide the direct measure of interfacial $Nd^{3+}$ coverages are very similar for salt and no-salt conditions over the same concentration range (Figure 2). Clearly, the presence of excess background ions helps $Nd^{3+}$ to dehydrate easily and interact with the headgroups, causing more significant changes in the SFG signal.

We hypothesize that the appearance of the 3150 $cm^{-1}$ peak in the -OH region around 1 mM bulk $Nd^{3+}$ is an indication of a majority of $Nd^{3+}$ ions being partially dehydrated and directly coordinating to the AA headgroups and the signal mainly originates from the first coordination shell of the $Nd^{3+}$ ions. XFNTR is not sensitive to the hydration state of the metal ion or its exact location next to the interface, while SFG does not directly detect the metal ion (Figure 1). We hypothesize that the changes in SFG spectra in the OH region are indicative of the changing interfacial hydration in response to the adsorption of the trivalent cations that have a strong hydration shell.[36] Using a combination of X-ray-based techniques and SFG, we have reported similar changes in interfacial hydration structures in response to adsorption of anionic complexes to positively charged surfaces.[8,28,29]

The formation of ion pairs in bulk solutions with multivalent ions has been shown to induce structural changes in the hydration layers.[39] Using Raman-difference spectroscopy, Patra et al. have shown that the first hydration layer of lanthanides has OH stretching modes that are red-shifted compared to those of bulk water.[40] In addition, they also report a peak at ∼3600 $cm^{-1}$ attributed to the second hydration shell. Our results for adsorption of Nd to the fatty acid monolayer qualitatively mirror the findings described above, supporting our hypothesis that the changes in OH spectra arise mainly due to metal-induced hydration changes.

As we focused on only AA/$Nd^{3+}$ systems here, we note that the surface structure and chemistry play an important role, and on mineral,[21] graphene,[22] and graphene oxide[41,42] surfaces, significantly different ion adsorption trends had been reported. Even the headgroup chemistry may lead to significant differences. For instance, phospholipid/$La^{3+}$ systems show clear signs of charge reversal in both X-ray- and SFG-based studies.[17,18] Specific interactions between the phosphate headgroup of DMPA and $La^{3+}$ were proposed as the cause of that overcharging effect. It is also interesting that Lee at al. observed overcharging of $Y^{3+}$ ions at the muscovite mica surface in the absence of any background salts and no overcharging with the NaCl background. This trend appears to be the opposite of our observation. We suggest that the surface structure and chemistry differences between mica and AA monolayers are responsible for this difference. The hydrophobicity of the air−water interface allows the “salting out” effect to dominate, while competition of $Na^+$ ions becomes important at the hydrophilic mica interface. However, a separate study is needed to elucidate the details.

The character of the trivalent ion may also be important in overcharging. Nd is a light lanthanide with a relatively larger ionic radius and, therefore, a lower charge density. Heavy lanthanides have smaller radii and therefore higher charge densities. In this study, we focused on Nd and showed that it does not induce overcharging. This does not rule out the possibility that heavy lanthanides lead to overcharging under similar conditions. For example, light and heavy lanthanides interact completely differently with DHDP, a phospholipid


https://doi.org/10.1021/acs.jpclett.3c00225
J. Phys. Chem. Lett. 2023, 14, 3685−3690

similar to DMPA but lacking the OH group. Although light lanthanides adsorb at DHDP monolayers without overcharging, heavier lanthanides cause the formation of inverted bilayers.[10,13]

The behavior of ions at charged interfaces is a central question in separation science, energy storage, and atmospheric chemistry. Due to the complexity inherent to the interfaces, a thorough description requires consolidation of results from various techniques that are sensitive to different aspects of the interfaces. Here we have shown the utility of combining SFG and X-ray fluorescence to investigate the structure of interfaces with adsorbed $Nd^{3+}$ ions next to negatively charged monolayers. We do not find any evidence of overcharging in the absence of the salt background, up to a $[Nd]_t$ of 1 mM, and consequently, we interpret the changes in the OH stretch region of SFG as indicators of changes in interfacial hydration due to lanthanide adsorption. There is XFNTR evidence of overcharging at 1 mM $[Nd]_t$ in the presence of 0.5 M NaCl. This shows that the OH region is sensitive to multiple factors with regard to ion adsorption and hydration and cannot be simply interpreted as a measure of ion adsorption or monolayer charge. We also demonstrated that the total coverage determined by X-ray studies is not enough to describe the interfacial distribution of the ions. Factors such as the background salts and surface functional groups may significantly affect the hydration of the ions, which in return can enhance or hinder ion transport in many applications. These results signify the need for a multiprong approach for addressing interfacial adsorption of ions to avoid overdrawn conclusions based on a single technique.

## ■ ASSOCIATED CONTENT

### Supporting Information

The Supporting Information is available free of charge at https://pubs.acs.org/doi/10.1021/acs.jpclett.3c00225.

Experimental methods, XFNTR data for $Nd^{3+}$ adsorption with and without NaCl, fit parameters for XFNTR data, and fit parameters for the $COO^-$ region via SFG with and without salt (PDF)

## ■ AUTHOR INFORMATION


### Corresponding Author

**Ahmet Uysal** − *Chemical Sciences and Engineering Division, Argonne National Laboratory, Lemont, Illinois 60439, United States;* orcid.org/0000-0003-3278-5570; Phone: +1-630-252-9133; Email: ahmet@anl.gov

### Authors

**Srikanth Nayak** − *Chemical Sciences and Engineering Division, Argonne National Laboratory, Lemont, Illinois 60439, United States;* orcid.org/0000-0003-0213-5796

**Raju R. Kumal** − *Chemical Sciences and Engineering Division, Argonne National Laboratory, Lemont, Illinois 60439, United States;* orcid.org/0000-0002-6077-8741

**Seung Eun Lee** − *Chemical Sciences and Engineering Division, Argonne National Laboratory, Lemont, Illinois 60439, United States;* orcid.org/0000-0002-5897-7266

Complete contact information is available at: https://pubs.acs.org/10.1021/acs.jpclett.3c00225


### Notes

The authors declare no competing financial interest.

## ■ ACKNOWLEDGMENTS

The authors thank Wei Bu for his assistance with the liquid surface synchrotron experiments. This work was supported by the U.S. Department of Energy (DOE), Office of Basic Energy Science, Division of Chemical Sciences, Geosciences, and Biosciences, Separation Science program, under Contract DE-AC02-06CH11357. Use of the Advanced Photon Source, an Office of Science User Facility operated for the DOE Office of Science by Argonne National Laboratory, was supported by the DOE under Contract DE-AC02-06CH11357. The National Science Foundation's ChemMatCARS Sector 15 is principally supported by the Divisions of Chemistry (CHE) and Materials Research (DMR) of the National Science Foundation under Grant NSF/CHE-1834750.

## ■ REFERENCES


(1) Hui, T. H.; Zhou, Z. L.; Qian, J.; Lin, Y.; Ngan, A. H. W.; Gao, H. Volumetric Deformation of Live Cells Induced by Pressure-Activated Cross-Membrane Ion Transport. *Phys. Rev. Lett.* **2014**, *113*, 118101.

(2) Magnussen, O. M.; Gross, A. Toward an Atomic-Scale Understanding of Electrochemical Interface Structure and Dynamics. *J. Am. Chem. Soc.* **2019**, *141*, 4777−4790.

(3) Sanchez-Fernandez, A.; Jackson, A. J.; Prévost, S. F.; Doutch, J. J.; Edler, K. J. Long-Range Electrostatic Colloidal Interactions and Specific Ion Effects in Deep Eutectic Solvents. *J. Am. Chem. Soc.* **2021**, *143*, 14158−14168.

(4) Testard, F.; Berthon, L.; Zemb, T. Liquid−Liquid Extraction: An Adsorption Isotherm at Divided Interface? *C. R. Chim.* **2007**, *10*, 1034−1041.

(5) Hu, Y.; Liu, Z.; Yuan, X.; Zhang, X. Molecular Mechanism for Liquid−Liquid Extraction: Two-Film Theory Revisited. *AIChE J.* **2017**, *63*, 2464−2470.

(6) Servis, M. J.; Clark, A. E. Surfactant-Enhanced Heterogeneity of the Aqueous Interface Drives Water Extraction into Organic Solvents. *Phys. Chem. Chem. Phys.* **2019**, *21*, 2866−2874.

(7) Miller, M.; Liang, Y.; Li, H.; Chu, M.; Yoo, S.; Bu, W.; Olvera de la Cruz, M.; Dutta, P. Electrostatic Origin of Element Selectivity During Rare Earth Adsorption. *Phys. Rev. Lett.* **2019**, *122*, 058001.

(8) Nayak, S.; Kumal, R. R.; Liu, Z.; Qiao, B. F.; Clark, A. E.; Uysal, A. Origins of Clustering of Metalate-Extractant Complexes in Liquid-Liquid Extraction. *ACS Appl. Mater. Interfaces* **2021**, *13*, 24194−24206.

(9) Sun, P.; Binter, E. A.; Liang, Z.; Brown, M. A.; Gelis, A. V.; Benjamin, I.; Bera, M. K.; Lin, B.; Bu, W.; Schlossman, M. L. Antagonistic Role of Aqueous Complexation in the Solvent Extraction and Separation of Rare Earth Ions. *ACS Cent. Sci.* **2021**, *7*, 1908−1918.

(10) Yoo, S.; Qiao, B. F.; Douglas, T.; Bu, W.; Olvera De la Cruz, M.; Dutta, P. Specific Ion Effects in Lanthanide-Amphiphile Structures at the Air-Water Interface and Their Implications for Selective Separation. *ACS Appl. Mater. Interfaces* **2022**, *14*, 7504−7512.

(11) Premadasa, U. I.; Ma, Y.-Z.; Sacci, R. L.; Bocharova, V.; Thiele, N. A.; Doughty, B. Understanding Self-Assembly and the Stabilization of Liquid/Liquid Interfaces: The Importance of Ligand Tail Branching and Oil-Phase Solvation. *J. Colloid Interface Sci.* **2022**, *609*, 807−814.

(12) Lin, L.; Liu, Z.; Premadasa, U. I.; Li, T.; Ma, Y.-Z.; Sacci, R. L.; Katsaras, J.; Hong, K.; Collier, C. P.; Carrillo, J.-M. Y.; Doughty, B. The Unexpected Role of Cations in the Self-Assembly of Positively Charged Amphiphiles at Liquid/Liquid Interfaces. *J. Phys. Chem. Lett.* **2022**, *13*, 10889−10896.

(13) Nayak, S.; Kumal, R. R.; Uysal, A. Spontaneous and Ion-Specific Formation of Inverted Bilayers at Air/Aqueous Interface. *Langmuir* **2022**, *38*, 5617−5625.

(14) Travesset, A.; Vaknin, D. Bjerrum Pairing Correlations at Charged Interfaces. *Europhys. Lett.* **2006**, *74*, 181−187.
(15) Misra, R. P.; de Souza, J. P.; Blankschtein, D.; Bazant, M. Z. Theory of Surface Forces in Multivalent Electrolytes. *Langmuir* **2019**, *35*, 11550−11565.
(16) Besteman, K.; Zevenbergen, M. A. G.; Heering, H. A.; Lemay, S. G. Direct Observation of Charge Inversion by Multivalent Ions as a Universal Electrostatic Phenomenon. *Phys. Rev. Lett.* **2004**, *93*, 170802.
(17) Sartin, M. M.; Sung, W.; Nihonyanagi, S.; Tahara, T. Molecular Mechanism of Charge Inversion Revealed by Polar Orientation of Interfacial Water Molecules: A Heterodyne-Detected Vibrational Sum Frequency Generation Study. *J. Chem. Phys.* **2018**, *149*, 024703.
(18) Pittler, J.; Bu, W.; Vaknin, D.; Travesset, A.; McGillivray, D. J.; Loesche, M. Charge Inversion at Minute Electrolyte Concentrations. *Phys. Rev. Lett.* **2006**, *97*, 046102.
(19) Chang, H.; Ohno, P. E.; Liu, Y.; Lozier, E. H.; Dalchand, N.; Geiger, F. M. Direct Measurement of Charge Reversal on Lipid Bilayers Using Heterodyne-Detected Second Harmonic Generation Spectroscopy. *J. Phys. Chem. B* **2020**, *124*, 641−649.
(20) Wang, W. J.; Park, R. Y.; Meyer, D. H.; Travesset, A.; Vaknin, D. Ionic Specificity in Ph Regulated Charged Interfaces: $Fe^{3+}$ Versus $La^{3+}$. *Langmuir* **2011**, *27*, 11917−11924.
(21) Lee, S. S.; Schmidt, M.; Laanait, N.; Sturchio, N. C.; Fenter, P. Investigation of Structure, Adsorption Free Energy, and Overcharging Behavior of Trivalent Yttrium Adsorbed at the Muscovite (001)-Water Interface. *J. Phys. Chem. C* **2013**, *117*, 23738−23749.
(22) Carr, A. J.; Lee, S. S.; Uysal, A. Trivalent Ion Overcharging on Electrified Graphene. *J. Condens. Matter Phys.* **2022**, *34*, 144001.
(23) Lee, S. S.; Koishi, A.; Bourg, I. C.; Fenter, P. Ion Correlations Drive Charge Overscreening and Heterogeneous Nucleation at Solid−Aqueous Electrolyte Interfaces. *Proc. Natl. Acad. Sci. U. S. A.* **2021**, *118*, e2105154118.
(24) Kumal, R. R.; Wimalasiri, P. N.; Servis, M. J.; Uysal, A. Thiocyanate Ions Form Antiparallel Populations at the Concentrated Electrolyte/Charged Surfactant Interface. *J. Phys. Chem. Lett.* **2022**, *13*, 5081−5087.
(25) Laanait, N.; Mihaylov, M.; Hou, B.; Yu, H.; Vanýsek, P.; Meron, M.; Lin, B.; Benjamin, I.; Schlossman, M. L. Tuning Ion Correlations at an Electrified Soft Interface. *Proc. Natl. Acad. Sci. U.S.A.* **2012**, *109*, 20326−20331.
(26) Sung, W.; Krem, S.; Kim, D. Binding of Trivalent Ions on Fatty Acid Langmuir Monolayer: Fe3+ Versus La3+. *J. Chem. Phys.* **2018**, *149*, 163304.
(27) Sthoer, A.; Adams, E. M.; Sengupta, S.; Corkery, R. W.; Allen, H. C.; Tyrode, E. C. La3+ and Y3+ Interactions with the Carboxylic Acid Moiety at the Liquid/Vapor Interface: Identification of Binding Complexes, Charge Reversal, and Detection Limits. *J. Colloid Interface Sci.* **2022**, *608*, 2169−2180.
(28) Kumal, R. R.; Nayak, S.; Bu, W.; Uysal, A. Chemical Potential Driven Reorganization of Anions between Stern and Diffuse Layers at the Air/Water Interface. *J. Phys. Chem. C* **2022**, *126*, 1140−1151.
(29) Rock, W.; Qiao, B. F.; Zhou, T. C.; Clark, A. E.; Uysal, A. Heavy Anionic Complex Creates a Unique Water Structure at a Soft Charged Interface. *J. Phys. Chem. C* **2018**, *122*, 29228−29236.
(30) Tyrode, E.; Corkery, R. Charging of Carboxylic Acid Monolayers with Monovalent Ions at Low Ionic Strengths: Molecular Insight Revealed by Vibrational Sum Frequency Spectroscopy. *J. Phys. Chem. C* **2018**, *122*, 28775−28786.
(31) Miller, M.; Chu, M. Q.; Lin, B. H.; Meron, M.; Dutta, P. Observation of Ordered Structures in Counterion Layers near Wet Charged Surfaces: A Potential Mechanism for Charge Inversion. *Langmuir* **2016**, *32*, 73−77.
(32) Wen, Y.-C.; Zha, S.; Liu, X.; Yang, S.; Guo, P.; Shi, G.; Fang, H.; Shen, Y. R.; Tian, C. Unveiling Microscopic Structures of Charged Water Interfaces by Surface-Specific Vibrational Spectroscopy. *Phys. Rev. Lett.* **2016**, *116*, 016101.
(33) Reddy, S. K.; Thiraux, R.; Wellen Rudd, B. A.; Lin, L.; Adel, T.; Joutsuka, T.; Geiger, F. M.; Allen, H. C.; Morita, A.; Paesani, F. Bulk Contributions Modulate the Sum-Frequency Generation Spectra of Water on Model Sea-Spray Aerosols. *Chem* **2018**, *4*, 1629−1644.
(34) Hunger, J.; Schaefer, J.; Ober, P.; Seki, T.; Wang, Y.; Prädel, L.; Nagata, Y.; Bonn, M.; Bonthuis, D. J.; Backus, E. H. G. Nature of Cations Critically Affects Water at the Negatively Charged Silica Interface. *J. Am. Chem. Soc.* **2022**, *144*, 19726−19738.
(35) Gonella, G.; Lütgebaucks, C.; de Beer, A. G. F.; Roke, S. Second Harmonic and Sum-Frequency Generation from Aqueous Interfaces Is Modulated by Interference. *J. Phys. Chem. C* **2016**, *120*, 9165−9173.
(36) Smith, D. W. Ionic Hydration Enthalpies. *J. Chem. Educ.* **1977**, *54*, 540−542.
(37) Sthoer, A.; Hladilkova, J.; Lund, M.; Tyrode, E. Molecular Insight into Carboxylic Acid-Alkali Metal Cations Interactions: Reversed Affinities and Ion-Pair Formation Revealed by Non-Linear Optics and Simulations. *Phys. Chem. Chem. Phys.* **2019**, *21*, 11329−11344.
(38) Backus, E. H. G.; Schaefer, J.; Bonn, M. Probing the Mineral−Water Interface with Nonlinear Optical Spectroscopy. *Angew. Chem., Int. Ed.* **2021**, *60*, 10482−10501.
(39) Roy, S.; Patra, A.; Saha, S.; Palit, D. K.; Mondal, J. A. Restructuring of Hydration Shell Water Due to Solvent-Shared Ion Pairing (Ssip): A Case Study of Aqueous Mgcl2 and Lacl3 Solutions. *J. Phys. Chem. B* **2020**, *124*, 8141−8148.
(40) Patra, A.; Roy, S.; Saha, S.; Palit, D. K.; Mondal, J. A. Observation of Extremely Weakly Interacting Oh (Similar to 3600 Cm(−1)) in the Vicinity of High Charge Density Metal Ions (Mz+; Z = 1, 2, 3): A Structural Heterogeneity in the Extended Hydration Shell. *J. Phys. Chem. C* **2020**, *124*, 3028−3036.
(41) Carr, A. J.; Lee, S. E.; Kumal, R. R.; Bu, W.; Uysal, A. Convenient Confinement: Interplay of Solution Conditions and Graphene Oxide Film Structure on Rare Earth Separations. *ACS Appl. Mater. Interfaces* **2022**, *14*, 57133−57143.
(42) Carr, A. J.; Kumal, R. R.; Bu, W.; Uysal, A. Effects of Ion Adsorption on Graphene Oxide Films and Interfacial Water Structure: A Molecular-Scale Description. *Carbon* **2022**, *195*, 131−140.


https://doi.org/10.1021/acs.jpclett.3c00225
J. Phys. Chem. Lett. 2023, 14, 3685−3690